Non-linear electrorheological instability of two streaming cylindrical fluids

2003 J. Phys. A: Math. Gen. 36 11343

(http://iopscience.iop.org/0305-4470/36/44/012)

INSTITUTE OF PHYSICS PUBLISHING JOURNAL OF PHYSICS A: MATHEMATICAL AND GENERAL

J. Phys. A: Math. Gen. **36** (2003) 11343–11365 PII: S0305-4470(03)62696-X

Non-linear electrorheological instability of two streaming cylindrical fluids

Galal M Moatimid

Department of Mathematics, Faculty of Education, Ain Shams University, Roxy, Cairo, Egypt

Received 22 April 2003, in final form 8 August 2003
Published 22 October 2003
Online at stacks.iop.org/JPhysA/36/11343

Abstract

A weakly non-linear instability of surface waves propagating through two viscoelastic cylindrical dielectric fluids is investigated. The examination is conducted in the presence of a tangential electric field and uniform axial relative streaming. The influence of the surface tension is taken into account, while the gravitational forces are ignored. Weak viscoelastic effects on the interface are considered, so that their contributions are demonstrated through the boundary conditions. Therefore, the equations of motion are solved in the absence of the viscoelastic effects. The solutions of the linearized equations of motion under the non-linear boundary conditions lead to derivation of a non-linear equation governing the interfacial displacement. This characteristic equation has damping terms and complex coefficients, where the nonlinearity is kept up to the third order. The linear state leads to a dispersion relation, where the stability is analysed. Taylor's theory is adopted to expand the governing non-linear equation in the light of the multiple scale technique, to impose the well-known Schrödinger equation. Several special cases are reported upon appropriate data choices. The stability criteria are discussed theoretically and illustrated graphically in which stability diagrams are obtained. Regions of stability and instability are identified for the electric field intensity versus the wave number for the wave train of the disturbance.

PACS numbers: 47.65.+a, 47.20.−k

1. Introduction

Electrohydrodynamics involves interactions between fluid motion and electrical field, customarily with non-polar, low-conductivity liquids known as leaky dielectrics. Electrorheological fluids are special viscous liquids that are characterized by their ability to undergo significant changes in their mechanical properties when an electric field is applied. This property can be exploited in technological applications, e.g. actuators, clutches and shock absorbers. Winslow [1] is credited with the first observation of the behaviour of electrorheological fluids in 1949. In recent years, a great deal of interest was focused on the understanding of the rheological effects occurring in the flow of non-Newtonian fluids. Now, this problem appears to be of special interest in oil reservoir engineering, where an increasing interest is shown in the possibility of improving oil recovery efficiency in water flooding projects through mobility control with non-Newtonian displacing fluids. Consequently, it has become essential to have an adequate understanding of the rheological effects of non-Newtonian displacing and displaced fluids in an oil displacement mechanism. Many technological processes involve the parallel flow of fluids of different viscosities, elasticities, densities and with different basic velocities. Such flows exist in packed bed reactors, in the chemical industry, petroleum engineering, plasma physics and in many other processes.

On the other hand, electrohydrodynamics is the field of the mechanics of continua that studies the motion of media interacting with electric field. Such an interaction takes place as a result of the action of the Coulomb force on a medium, or as a result of the work of the electric field in the flow of currents. The motion of a medium gives rise to re-distribution of a volume charge, which results in a change of the electric field and, hence, the force acting on a medium. Applications of electrohydrodynamics in various diverse fields have great interest. Some of these applications are electrified fluid dynamics of biological systems, dielectrophoretic orientation and expulsion of liquids in zero gravity environment, and insulation research in liquids and gases. There seems to be a close connection between this area and atmospheric and cloud physics, physicochemical hydrodynamics, bubble and drop dynamics, and the electrostatics of thunderstorms. In view of these facts, there is a growing need for original research in basic electrohydrodynamic phenomena on which the spectrum of applications is based [2–4].

The non-Newtonian fluids have gained increasing technological applications. They are considered more realistic compared to the Newtonian fluids. Of particular interest is the class of fluids known as viscoelastic fluids which exhibit the properties of elasticity besides those of viscosity. The study of viscoelastic fluids has become of increasing importance in the last few years. This is mainly due to their various applications in petroleum drilling, manufacturing of foods and paper, and many similar activities. The surface between two fluids is of special importance owing to its applications to many engineering problems. A generalization of the Kelvin–Helmholtz instability for viscoelastic flow is a very difficult problem. The difficulty arises as the two viscoelastic fluids are in relative motion. In order to solve the problem of viscous flow, Feng and Beard [5] restrict themselves to the case of weak viscous effects. This weakness is regarded such that viscous effects appear at the interface and gradually decrease to be negligible at the bulk [5–8], and the contribution will be demonstrated in the boundary conditions. A most recent work on this topic is introduced by Moatimid [9]. His system is composed of a streaming dielectric fluid sheet of finite thickness embedded between two different streaming finite dielectric fluids. The interfaces permit mass and heat transfer. His analysis reveals that the sheet thickness and mass and heat transfer parameters have a dual influence on the stability picture, especially at small values of the wave number. He applied the Feng and Beard [5] treatment, where the viscous contribution has been demonstrated through the normal stress tensor boundary condition. The linear electrohydrodynamic Kelvin–Helmholtz instability of two superposed Rivlin–Ericksen viscoelastic fluids was investigated by El-Sayed [10]. His numerical results showed that Stokes drag coefficient, electric field and kinematical viscosity have destabilizing effects. El-Dabe *et al* [11] investigated the problem of heat and mass transfer due to the steady motion of a Rivlin–Ericksen fluid in a tube of varying cross sections. Under the assumption that the deformations of the boundaries are small, they solved the equations of motion by a perturbation technique.

Several authors carried out non-linear analysis using the method of multiple scale expansion. Nayfeh [12] studied the stability of a non-linear surface wave propagating through a horizontal interface between two inviscid fluids. A most recent work on this topic is studied by Moatimid [13]. He analyses linear and non-linear stability aspects for flow of parallel streaming magnetic fluids through a porous medium confined between parallel walls. Allowance is made for heat transfer and phase change mass transfer across the interface of the fluids. He obtained a Ginzburg–Landau equation, describing the behaviour of the system through a non-linear approach. Because of the wide practical applications of the stability analysis of the cylindrical interface, many authors worked in this area. Othman [14] investigated the electrohydrodynamic instability of a cylindrical interface. In his analysis, at the critical point, a generalized formulation of the evolution equation is developed and leads to the non-linear Klein–Gordon equation. The non-linear stability of magnetic fluids of cylindrical interface with mass and heat transfer was studied by Lee [15]. His analysis, based on multiple scales method, shows that the evolution of the amplitude is governed by a non-linear Ginzburg–Landau equation. He found the various stability criteria, where the region of stability is displayed graphically. The non-linear stability of a cylindrical interface with mass and heat transfer in magnetic fluids was investigated by Lee [16]. He showed that the non-linear effect can increase the stability range when there is strong heat and mass transfer. He also found that, with the strong magnetic field, the system is more stable. A non-linear break-up of a fluid jet forming a plane sheet and stressed at the surface by an electric field was studied by Lee [17]. He applied the method of strained coordinates for studying the capillary instability of the jet. He also obtained the time of break-up of the jet numerically. Recent works on the non-linear instability of cylindrical structures of finitely conducting fluids under the influence of electric fields in different situations can be found in Elhefnawy *et al* [18–20]. In their analysis, which is based on multiple scale technique, two non-linear Schrödinger and Klein–Gordon equations are derived. They discussed the modulation instability of a finite wave train solution and compared with the linear instability theory. They found new instability regions in the parameter space, which appear due to the non-linear effects.

Several researchers have already studied the hydrodynamic stability problems regarding the fluid films flowing down a vertical cylinder surface. Rosenau and Oron [21] derived an amplitude equation which describes the evolution of a disturbed free film surface travelling down an infinite vertical cylindrical column. The numerical modelling results indicated that both conditions of supercritical stability and subcritical instability can occur for the film flow. The results also showed that the evolving waves may break the moment linearly unstable conditions are satisfied. Davalos-Orozco and Ruiz-Chavarria [22] investigated the linear stability of a fluid layer flowing down inside and outside a rotating vertical cylinder. They pointed out that the centrifugal force could stabilize the film flow so as to counteract the destabilizing effect of surface tension. In the absence of rotation, the stability can still be found for some critical wave numbers. Hung *et al* [23] investigated the weakly non-linear stability analysis of condensation film flowing through a vertical cylinder. They showed that supercritical stability and subcritical instability in the linear unstable region can coexist. They also indicated that the lateral curvature of the cylinder has destabilizing effect on the film flow instability. Cheng *et al* [24] investigated the weakly non-linear stability theory of a thin micropolar liquid film flowing down along the outside surface of a vertical cylinder. They employed the long-wave perturbation method to solve the generalized non-linear kinematic equations with free film interface. First, they used the normal mode approach to analyse the linear stability of the free film interface. Second, they used the method of multiple scales to obtain the weak non-linear dynamics of the film flow for stability analysis. Their modelling results indicated that both subcritical instability and supercritical stability conditions can occur in a microploar film flow system.

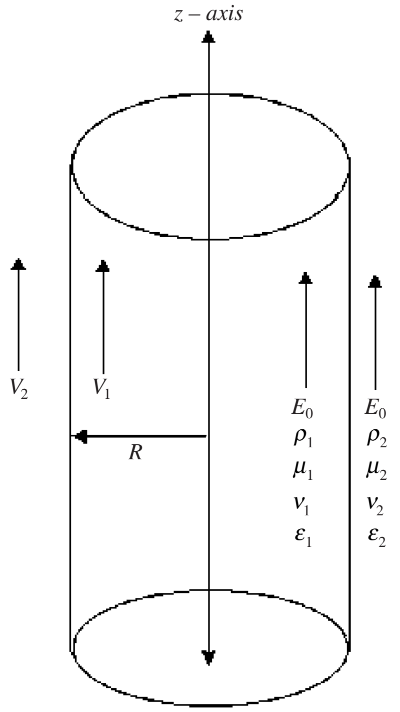

Figure 1. Sketch of the system under consideration.

Because of the several practical applications of the viscoelastic cylindrical fluids, the present work is concerned with simple viscoelastic cylindrical flows with uniform relative velocities. A generalization of the non-linear streaming instability for the Rivlin–Ericksen flow under the effect of an axial electric field is the aim of this study. Through the following analysis, viscoelastic contributions will be demonstrated through the boundary conditions. However, one must address some additional complexities that principally arise due to the interaction between the viscoelastic fluids with the electric field through the non-linear analysis. In this work, we have concentrated on a weak non-linear scheme that is based on the idea of linear solutions under the non-linear boundary conditions. The main purpose is to discuss modulation instability of a finite wave train solution and compare the results with the linear instability theory. The scheme of the model is presented as follows. In section 2, we formulate the configuration of the problem, where the basic equations with the accompanying boundary conditions are introduced. The non-linear characteristic equation of the surface evolution is obtained in section 3. Section 4 is devoted to the display of the linear problem as a limiting case with its special cases. The non-linear approach is introduced in section 5 for deriving the Ginzburg–Landau equation. Finally, the outlines of the problem are added as concluding remarks in section 6.

2. Formulation of the problem

The considered system is specifically associated with the stability problems. A parallel flow of two immiscible viscoelastic fluids in infinite, fully saturated, uniform and homogeneous media is shown in figure 1. The two fluids are incompressible and have uniform properties. The interface between the two fluids is assumed to be well defined and initially cylindrical.

The fluids are assumed to have a viscoelastic nature described by the following constitutive relation:

$$\sigma_{ij}^{\text{hydro.}} = -p\delta_{ij} + \left[\mu + \nu\left(\frac{\partial}{\partial t} + v_k\frac{\partial}{\partial x_k}\right)\right]\left(\frac{\partial v_i}{\partial x_j} + \frac{\partial v_j}{\partial x_i}\right) \tag{2.1}$$

where $\sigma_{ij}^{\text{hydro.}}$ is the hydrodynamic stress tensor, δ_{ij} is the Kronecker delta, p is the hydrostatic pressure, μ is the viscosity coefficient, ν is the viscoelastic coefficient and $\underline{v}$ is the fluid velocity vector.

Gravity forces are assumed to be ignored. The cylindrical polar coordinates (r, θ, z) are considered. In the equilibrium state, the z-axis is the axis of symmetry of the system. The inner and outer fluids have densities ρ_1 and ρ_2 and dielectric constants ε_1 and ε_2, respectively. Generally, the subscripts 1 and 2 refer to the inner and outer fluids, respectively. The two fluids stream with uniform velocities V_1 and V_2 along the positive z-direction. It is also assumed that the jet is acted upon by the influence of a uniform axial electric field E_0 along the axis of the jet. There are no volume charges in the fluid layers. In addition, no free surface charges are present at the interface between the two fluids.

The electric Maxwell stress tensor [25] is given by

$$\sigma_{ij}^{\text{elect.}} = \varepsilon E_i E_j - \tfrac{1}{2}\varepsilon E^2\delta_{ij}. \tag{2.2}$$

At the initial state of the system, we assume that both fluid phases are immiscible and have a common cylindrical interface at $r = R$. The distribution equilibrium of the interface between both electrified fluid phases has been established. Due to the very intricate nature of the problem of the streaming flow of non-Newtonian dielectric cylindrical fluids, we confine our analysis to the consideration of weak viscoelastic effects. The introduction of the weak viscous effects is customary in the case of a Newtonian fluid [5–7] and should be understood in a manner similar to a viscoelastic problem, which makes problem formulation much easier to handle. Moreover, the same technique has been successfully applied to viscoelastic fluid of Maxwellian type in the linear perturbation theory by El-Dib and Moatimid [8]. Therefore, in order to make use of the domain perturbation technique, we confine the analysis to the consideration of weak viscoelastic effects which are believed to be significant only within a thin vortical surface layer, so that the motions elsewhere in the bulk may be reasonably assumed irrotational. The viscoelastic effects are incorporated by a novel method of formulating a normal damping stress term in the boundary condition at the interface, based on the assumption that the overall rate of work done by this damping stress equals the total rate of dissipation of mechanical energy as presented in Batchelor [26]. Thus the derivations in this problem deal completely with potential flow so that the complicated manipulation of the boundary layer equations for the weak vortical flow can be avoided. Since the equations governing the irrotational flow is the Laplace equation, modification of the boundary conditions at the interface should be acceptable, which means inclusion of the small viscoelastic effects. At this end, in the present study, the viscoelastic effects may be formulated through the normal stress boundary conditions. Therefore, in view of the viscoelastic approximation, the governing equations in the bulk of the fluid phases are given by

$$\rho\left[\frac{\partial \underline{v}}{\partial t} + (\underline{v}\,.\,\underline{\nabla})\underline{v}\right] = -\nabla p \tag{2.3}$$

and the incompressibility condition

$$\nabla\,.\,\underline{v} = 0. \tag{2.4}$$

We are interested in the interfacial response between two cylindrical fluids after a disturbance about the equilibrium configuration. Therefore, the surface deflection is expressed by $r = R + \eta$, where

$$\eta = \gamma\, \mathrm{e}^{\mathrm{i}(kz+m\theta-\omega t)} + \mathrm{c.c.} \tag{2.5}$$

Here, γ is an arbitrary parameter, which determines the behaviour of the amplitude of the disturbance. Through the linear theory, the amplitude is assumed to be constant. On the other hand, along the non-linear approach, γ is treated as a slowly varying function of space and time. In addition, k is the axial wave number, which is assumed to be real and positive, m is the azimuthal wave number, which is assumed to be positive integer, ω is the growth rate and c.c. refers to the complex conjugate of the preceding term. It should be noted that the imaginary part of ω indicates a disturbance that either grows with time (instability) or decays with time (stability), depending on whether this imaginary part is positive or negative, respectively. As shown by many foregoing works, e.g. Chandrasekhar [27], the liquid jet is stable for all purely non-axisymmetric deformations, but is unstable for symmetric varicose deformations with wavelengths exceeding the circumference of the cylinder. It follows that the most interesting mode of disturbance is the axisymmetric mode. Therefore, from now on, the axisymmetric mode ($m = 0$) is only considered. We define a function $\Upsilon(r, z; t) = r - R - \gamma\, \mathrm{e}^{\mathrm{i}(kz-\omega t)}$, where $\Upsilon(r, z; t) = 0$ describes the wave-like profile of the disturbed interface. So, the disturbed interface is located at $r = R + \gamma\, \mathrm{e}^{\mathrm{i}(kz-\omega t)}$ and the outward unit normal vector to that interface is given by

$$\underline{n} = (\underline{e}_r - \mathrm{i}k\eta\underline{e}_z)(1 - k^2\eta^2)^{-\frac{1}{2}} \tag{2.6}$$

where $\underline{e}_r$ and $\underline{e}_z$ are the unit vectors along r- and z-directions, respectively.

To examine the interfacial stability of the flow under consideration, two-dimensional finite disturbances are introduced into the equations of motion as well as the boundary conditions. By two-dimensional finite disturbance, we mean that the flow depends on the horizontal direction of propagation, i.e. the r-direction and the vertical z-direction. As a result of perturbation, the initial fluid velocity increases and allows the introduction of the potential function $\phi(r, z, t)$ such that the total velocity is defined as

$$\underline{v}_j = V_j\underline{e}_z + \nabla\phi_j \qquad j = 1, 2. \tag{2.7}$$

For an incompressible fluid, we find that the potential ϕ_j satisfies the following Laplace equations.

$$\nabla^2\phi_1 = 0 \qquad r \leqslant R + \eta \tag{2.8}$$

$$\nabla^2\phi_2 = 0 \qquad r \geqslant R + \eta. \tag{2.9}$$

The electrically insulating fluid justifies the stationary form of the Maxwell equations, which are reduced to the Laplace equation for the electric potential $\psi_j(r, z; t)$ in each of the two cylindrical fluids. The scalar electric potentials are defined as

$$\underline{E}_j = E_0\underline{e}_z - \nabla\psi_j \qquad j = 1, 2. \tag{2.10}$$

It follows that the potential ψ_j has to satisfy Laplace's equations

$$\nabla^2\psi_1 = 0 \qquad r \leqslant R + \eta \tag{2.11}$$

$$\nabla^2\psi_2 = 0 \qquad r \geqslant R + \eta. \tag{2.12}$$

The solutions of the equations of motion cited above are accomplished by utilizing the convenient boundary conditions. At the boundary between the two cylindrical fluids, the fluids and the electrical stresses must be balanced. The components of these consist of the hydrodynamic pressure, viscoelastic stresses, surface tension and electric stresses. The electric stresses result from the dielectric forces [25].

At the fluid interface, it is required that both the horizontal and vertical components of the fluid velocity satisfy an equation expressing the assumed material character of the dividing surface. This is the so-called kinematical boundary condition, which gives

$$\frac{\partial\eta}{\partial t} - \frac{\partial\phi_j}{\partial r} + \frac{\partial\eta}{\partial z}\left(V_j + \frac{\partial\phi_j}{\partial z}\right) = 0 \qquad j = 1, 2. \tag{2.13}$$

On the other hand, for the electric part, the jump in the tangential components of the electric field is zero across the interface, which leads to

$$\frac{\partial\eta}{\partial z}\left\|\frac{\partial\psi}{\partial r}\right\| + \left\|\frac{\partial\psi}{\partial z}\right\| = 0 \tag{2.14}$$

where

$$\|f\| = f_1 - f_2.$$

In addition, since there are no surface charges, the normal electric displacement is continuous at the interface, which requires

$$\left\|\varepsilon\frac{\partial\psi}{\partial r}\right\| - \frac{\partial\eta}{\partial z}\left\|\varepsilon\frac{\partial\psi}{\partial z}\right\| + \|\varepsilon\|E_0\frac{\partial\eta}{\partial z} = 0. \tag{2.15}$$

The remaining boundary condition arises from the normal component of the stress tensor σ_{ij}. This component is discontinuous, at the interface, because of surface tension. This may be formulated as follows:

$$\underline{n}\|\underline{F}\| = T\left(\frac{1}{R_1} + \frac{1}{R_2}\right) \tag{2.16}$$

where $\underline{F}$ is the total force acting on the interface, which is defined as

$$\underline{F} = \begin{pmatrix}\sigma_{rr} & \sigma_{rz}\\ \sigma_{zr} & \sigma_{zz}\end{pmatrix}\begin{pmatrix}n_r\\ n_z\end{pmatrix} \tag{2.17}$$

T represents the surface tension coefficient, R_1 and R_2 are the two principle radii of curvature, and n_r and n_z are the components of the unit vector $\underline{n}$, and

$$\sigma_{ij} = \sigma_{ij}^{\text{hydro.}} + \sigma_{ij}^{\text{elect.}}$$

The normal stress tensor (2.16), eliminating the pressure by Bernoulli's equation, may be expanded as follows:

$$\begin{aligned}
&\left\|\rho\frac{\partial\phi}{\partial t}\right\| + \left\|\rho V\frac{\partial\phi}{\partial z}\right\| - T\left[\frac{\eta}{R^2} - k^2\eta - \frac{\eta^2}{R^3} + \frac{\eta^3}{R^4} - \frac{1}{2}k^2\eta^2\left(\frac{1}{R} - \frac{\eta}{R^2} + 3k^2\eta\right)\right]\\
&\qquad + (1 + k^2\eta^2)\|\tau_{rr} - 2\mathrm{i}k\tau_{rz} - k^2\eta^2\tau_{zz}\|\\
&\quad = -E_0\left\|\varepsilon\frac{\partial\psi}{\partial z}\right\| + \frac{1}{2}\left\|\varepsilon\left[\left(\frac{\partial\psi}{\partial z}\right)^2 - \left(\frac{\partial\psi}{\partial r}\right)^2\right]\right\| + k^2\eta^2E_0\|\varepsilon\|\\
&\qquad - 2\mathrm{i}k\eta E_0\left\|\varepsilon\frac{\partial\psi}{\partial r}\right\| + 2\mathrm{i}k\eta\left\|\varepsilon\frac{\partial\psi}{\partial r}\frac{\partial\psi}{\partial z}\right\| - 2k^2\eta^2E_0\left\|\varepsilon\frac{\partial\psi}{\partial z}\right\|
\end{aligned} \tag{2.18}$$

where

$$\tau_{rr} = 2\mu\frac{\partial^2\phi}{\partial r^2} + 2\nu\left[\frac{\partial^3\phi}{\partial t\partial r^2} + \frac{\partial\phi}{\partial r}\frac{\partial^3\phi}{\partial r^3} + \left(V + \frac{\partial\phi}{\partial z}\right)\frac{\partial^3\phi}{\partial z\partial r^2}\right]$$

$$\tau_{rz} = 2\mu\frac{\partial^2\phi}{\partial r\partial z} + 2\nu\left[\frac{\partial^3\phi}{\partial t\partial r\partial z} + \frac{\partial\phi}{\partial r}\frac{\partial^3\phi}{\partial z\partial r^2} + \left(V + \frac{\partial\phi}{\partial z}\right)\frac{\partial^3\phi}{\partial r\partial z^2}\right]$$

and

$$\tau_{zz} = 2\mu\frac{\partial^2\phi}{\partial z^2} + 2\nu\left[\frac{\partial^3\phi}{\partial t\partial z^2} + \frac{\partial\phi}{\partial r}\frac{\partial^3\phi}{\partial r\partial z^2} + \left(V + \frac{\partial\phi}{\partial z}\right)\frac{\partial^3\phi}{\partial z^3}\right].$$

Now, we will proceed to derive the non-linear characteristic equation, governing the surface evolution. Keeping in mind that the elevation function η is small, we maintain only the third-order terms.

3. The non-linear characteristic equation

The analysis of the linear stability as presented by Chandrasekhar [27] is based on neglecting the non-linear terms from the equations of motion as well as the boundary conditions. Therefore, a dispersion relation should arise without non-linear terms. The idea for the weak non-linear approach is a slight departure from the linearity technique. At this stage, the whole problem will contain the linear dispersion with some additional terms that make a correction of the main solution. The weak non-linear description given here is based on neglecting the non-linear terms from the equations of motion and application of the appropriate non-linear boundary conditions. Therefore, the dispersion relation should be extended to include the non-linear terms.

To solve the linearized equations of motion for the system under consideration, two-dimensional finite disturbances are introduced to this boundary-value problem. As is customary in hydrodynamic stability theory [27], all perturbed physical quantities have exponential time dependence and a periodic spatial dependence. Also, in view of the standard Fourier decomposition, we may similarly assume that the bulk solutions are in the form

$$\phi_j(r, z; t) = \hat{\phi}_j(r)\,\mathrm{e}^{\mathrm{i}(kz-\omega t)} \qquad j = 1, 2 \tag{3.1}$$

$$\psi_j(r, z; t) = \hat{\psi}_j(r)\,\mathrm{e}^{\mathrm{i}(kz-\omega t)} \qquad j = 1, 2 \tag{3.2}$$

where $\hat{\phi}_j(r)$ and $\hat{\psi}_j(r)$ are arbitrary functions of r.

Substituting equation (3.1) into equations (2.8) and (2.9), the solutions which are consistent with the non-linear boundary condition (2.13) are related to the interfacial displacement η as

$$\phi_1(r, z; t) = \frac{\mathrm{i}(kV_1 - \omega)I_0(kr)\eta}{k(I_1(kR) + k\eta I_0(kR))} \qquad r \leqslant R + \eta(z, t) \tag{3.3}$$

$$\phi_2(r, z; t) = -\frac{\mathrm{i}(kV_2 - \omega)K_0(kr)\eta}{k(K_1(kR) - k\eta K_0(kR))} \qquad r \geqslant R + \eta(z, t). \tag{3.4}$$

The above distributions of the velocity potential function $\phi_1(r, z; t)$ and $\phi_2(r, z; t)$ contain non-linear terms in the elevation parameter η. This non-linearity occurs because of the use of the non-linear boundary condition (2.13). As the non-linear terms are ignored, a linear profile arises and is equivalent to those obtained by Moatimid [28].

Again, inserting equation (3.2) into equations (2.14) and (2.15), one gets

$$\psi_1(r, z; t) = \frac{\mathrm{i}E_0}{\Delta}(\varepsilon_2 - \varepsilon_1)(K_0(kR) - k\eta K_1(kR))I_0(kr)\eta \tag{3.5}$$

$$\psi_2(r, z; t) = \frac{\mathrm{i}E_0}{\Delta}(\varepsilon_2 - \varepsilon_1)(I_0(kR) - k\eta I_1(kR))K_0(kr)\eta \tag{3.6}$$

where

$$\Delta = \varepsilon_1[(I_1(kR) + k\eta I_0(kR))(K_0(kR) - k\eta K_1(kR))] + \varepsilon_2[(I_0(kR) + k\eta I_1(kR))(K_1(kR) - k\eta K_0(kR))]$$

(I_0, I_1) and (K_0, K_1) are the modified Bessel functions of the first and second kinds, respectively.

The above distributions of the scalar electric potential $\psi_1(r, z; t)$ and $\psi_2(r, z; t)$ contain non-linear terms in the elevation parameter η. As the non-linear terms are ignored, a linear profile arises.

Inserting equations (3.3)–(3.6) into the normal stress tensor (2.18), the scalar electric potential $\psi_j(r, z; t)$ and the velocity potential $\phi_j(r, z; t)$ are replaced by their equivalence in terms of the elevation parameter η. The result is a very complicated non-linear equation in the elevation η. Keeping in mind that the elevation function η is small, the use of the binomial expansion is convenient. The calculations are lengthy but straightforward. Up to the third order of η, one finds the following non-linear equation in the interfacial displacement η:

$$S(\omega, k)\eta = \alpha(\omega, k)\eta^2 + \beta(\omega, k)\eta^3 + \cdots \tag{3.7}$$

where

$$\begin{aligned} S(\omega, k) = {} & [\rho_1 M_0(kR) + \rho_2 N_0(kR) + k^2(\nu_1(M_0(kR) + M_2(kR)) + \nu_2(N_0(kR) + N_2(kR)))]\omega^2 \\ & + [-2k(V_1(k^2\nu_1(M_0(kR) + M_2(kR)) + \rho_1 M_0(kR)) + V_2(k^2\nu_2(N_0(kR) \\ & + N_2(kR)) + \rho_2 N_0(kR))) + \mathrm{i}k^2(\mu_1(M_0(kR) + M_2(kR)) + \mu_2(N_0(kR) \\ & + N_2(kR)))]\omega + \frac{kT}{R^2}(1 - k^2R^2) - k^2E_1(kR)E_0^2 + k^2\big[V_1^2(k^2\nu_1(M_0(kR) \\ & + M_2(kR)) + \rho_1 M_0(kR)) + V_2^2(k^2\nu_2(N_0(kR) + N_2(kR)) + \rho_2 N_0(kR))\big] \\ & - \mathrm{i}k^3[\mu_1 V_1(M_0(kR) + M_2(kR)) + \mu_2 V_2(N_0(kR) + N_2(kR))] \end{aligned}$$

$\alpha(\omega, k)$ and $\beta(\omega, k)$ are given in appendix A.

The terms $\alpha(\omega, k)$ and $\beta(\omega, k)$ denote the coefficients of the second- and third-order terms, respectively, of the characteristic equation (3.7). These non-linear terms are obtained due to the use of the non-linear boundary conditions cited above. According to the general theory of Grimshaw [29], the non-linear terms of the characteristic equation (3.7) consist of two terms. One part contains the interaction of the second harmonic term, together with the cubic interaction of the primary harmonic term, which is identical to the same term that arises in the Stokes expansion for a plane progressive wave. Indeed, equation (3.7) is more general than that obtained by several authors using the linear theory.

4. The linear stability approach

The goal here is to analyse the stability of the problem at hand throughout a linear approach. In the linear analysis, the linear curve leads to an understanding of the mechanism of the jet break-up. That is the formation of the main (parent) drops, which occurs in the unstable region. The phenomenon of break-up provides a mechanism for the production of fine sprays. The process has many practical applications, for example in paint spraying and crop spraying. To accomplish the linear analysis of the considered system, the linearized form of equation (3.7) should arise when higher orders of η are ignored. At this stage, equation (3.7) is reduced to

$$S(\omega, k)\eta = 0 \tag{4.1}$$

where $S(\omega, k)$ represents the linear dispersion function, corresponding to the linear dispersion relation

$$L\left(\frac{\partial}{\partial t}, \frac{\partial}{\partial z}\right)\eta = 0. \tag{4.2}$$

L is a linear operator involving the partial derivatives $\frac{\partial}{\partial t}$, $\frac{\partial}{\partial z}$. We first study equation (4.2) and then return to equation (3.7) to incorporate the higher order dispersive effects. We require a uniform monochromatic wave train solution to equation (3.7) in the light of equations (3.1) and (3.2). The existence of harmonic wave trains in the dispersive medium and the correspondence between the wave number and frequency lead to several physical consequences. Now, equation (4.2) may be written as

$$L(-\mathrm{i}\omega, \mathrm{i}k)\eta = 0. \tag{4.3}$$

It follows that from equation (4.1), as $\eta \neq 0$, we have

$$a_0\omega^2 + (a_1 + \mathrm{i}b_1)\omega + (a_2 + \mathrm{i}b_2) = 0 \tag{4.4}$$

where

$$\begin{aligned}
a_0 &= \rho_1 M_0(kR) + \rho_2 N_0(kR) + k^2[\nu_1(M_0(kR) + M_2(kR)) + \nu_2(N_0(kR) + N_2(kR))] \\
a_1 &= -2k[V_1(k^2\nu_1(M_0(kR) + M_2(kR)) + \rho_1 M_0(kR)) \\
&\qquad + V_2(k^2\nu_2(N_0(kR) + N_2(kR)) + \rho_2 N_0(kR))] \\
b_1 &= k^2[\mu_1(M_0(kR) + M_2(kR)) + \mu_2(N_0(kR) + N_2(kR))] \\
a_2 &= \frac{kT}{R^2}(1 - k^2R^2) + k^2\big[\big(V_1^2(k^2(M_0(kR) + M_2(kR))\nu_1 + M_0(kR)\rho_1\big) \\
&\qquad + V_2^2(k^2(N_0(kR) + N_2(kR))\nu_2 + K\rho_2))\big] - k^2E_1(kR)E_0^2 \\
b_2 &= -k^3[\mu_1 V_1(M_0(kR) + M_2(kR)) + \mu_2 V_2(N_0(kR) + N_2(kR))].
\end{aligned}$$

It should be noted that equation (4.4) represents the linear dispersion relation for surface waves propagating through two cylindrical streaming Rivlin–Ericksen fluids. This dispersion relation is satisfied by the values of ω and k. That is, if the real part of ω is positive, the disturbance will grow in time and the basic flow (V_1, V_2) becomes unstable. On the other hand, if the real part of ω is negative, the disturbance will decay and the basic flow will be stable.

Before dealing with the dispersion relation (4.4), it is convenient to consider the following special cases:

[i] *Pure inviscid jet* $(\mu_1 = \mu_2 = \nu_1 = \nu_2 = 0)$. In this case equation (4.4) reduces to

$$a_0^*\omega^2 + a_1^*\omega + a_2^* = 0 \tag{4.5}$$

where a_0^*, a_1^* and a_2^* have the same definitions as a_0, a_1 and a_2 but is the case of a pure inviscid jet.

From (4.5), we find that the system is stable if $a_1^{*2} - 4a_0^*a_2^* \geqslant 0$, or

$$E_1(kR)E_0^2 + \frac{T}{kR^2}(k^2R^2 - 1) - \frac{\rho_1\rho_2 M_0(kR)N_0(kR)(V_1 - V_2)^2}{\rho_1 M_0(kR) + \rho_2 N_0(kR)} \geqslant 0. \tag{4.6}$$

It is apparent from inequality (4.6) that a uniform axial electric field and surface tension have strictly stabilizing effects while the streaming difference has an opposite influence. In the absence of the electric field, inequality (4.6) reduces to Rayleigh criterion [30] for the hydrodynamic jet whose maximum growth of instability occurs at $k = 0.678$ for $R = 1$ and stability occurs when $kR > 1$.

Before considering the numerical calculations, it is convenient to write the stability conditions in an appropriate dimensionless form. This can be done in a number of ways depending primarily on the choice of the characteristic length. Consider the following dimensionless forms: the characteristic length $= R$, the characteristic time $= \frac{1}{\omega}$ and the characteristic mass= $\frac{T}{\omega^2}$. The other dimensionless quantities are given by

$$k = \frac{k^*}{R} \qquad \rho_j = \rho_j^* \frac{T}{\omega^2 R^3} \qquad V_j = V_j^* R\omega \qquad E_0^2 = E_0^{*2} \frac{T}{R}$$
$$\mu_j = \mu_j^* \frac{T}{\omega R} \qquad \text{and} \qquad \nu_j = \nu_j^* \frac{T}{\omega^2 R} \qquad j = 1, 2 \tag{4.7}$$

where the superposed asterisks refer to dimensionless quantities. From now on, it will be omitted for simplicity. To this end, the interface of the system becomes stable or unstable depending on whether the electric field intensity E_0^2 is larger or smaller than E_{C1}, where

$$E_{C1} = \frac{1}{E_1(k)} \left[\frac{1}{k} - k + \frac{\rho_1 \rho_2 M_0(k) N_0(k) (V_1 - V_2)^2}{\rho_1 M_0(k) + \rho_2 N_0(k)} \right]. \tag{4.8}$$

[ii] *When the viscosity coefficients* μ_1 *and* μ_2 *are ignored.* This case deals with the influence of the viscoelastic coefficients only. Equation (4.4) then reduces to

$$\hat{a}_0 \omega^2 + \hat{a}_1 \omega + \hat{a}_2 = 0 \tag{4.9}$$

where $\hat{a}_0, \hat{a}_1$ and $\hat{a}_2$ have the same definitions as a_0, a_1 and a_2 but when $\mu_1 = \mu_2 = 0$. In this case, the stability condition becomes

$$E_0^2 \geqslant E_{C2} \tag{4.10}$$

$$E_{C2} = \frac{1}{E_1(k)} \left[\frac{1}{k} - k + \frac{(V_1 - V_2)^2 (C_{21} + C_{22})}{C_{21} + C_{22}} \right]$$
$$C_{21} = k^2 \nu_1 (M_0(k) + M_2(k)) + \rho_1 M_0(k)$$

and

$$C_{22} = k^2 \nu_2 (N_0(k) + N_2(k)) + \rho_2 N_0(k).$$

[iii] *When the two cylindrical fluids have no viscoelastic coefficients* ($\nu_1 = \nu_2 = 0$). Therefore, the motion is restricted by the viscosity coefficients only. In this case, equation (4.4) becomes

$$\tilde{a}_0 \omega^2 + (\tilde{a}_1 + \mathrm{i}\tilde{b}_1)\omega + (\tilde{a}_2 + \mathrm{i}\tilde{b}_2) = 0 \tag{4.11}$$

where $\tilde{a}_0, \tilde{a}_1, \tilde{a}_2, \tilde{b}_1$ and $\tilde{b}_2$ have the same definitions as a_0, a_1, a_2, b_1 and b_2 but when $\nu_1 = \nu_2 = 0$.

It is well known from the Routh–Hurwitz criterion [31] that the necessary and sufficient stability conditions for equation (4.11) (in other words, to have the imaginary part of ω either less than or equal to zero) are

$$\tilde{a}_0 \tilde{b}_2^2 - \tilde{a}_1 \tilde{b}_1 \tilde{b}_2 + \tilde{a}_2 \tilde{b}_1^2 \leqslant 0 \tag{4.12}$$

since $\tilde{a}_0$ and $\tilde{b}_1$ are always positive.

It follows that the system is linearly stable when

$$E_0^2 \geqslant E_{C3} \tag{4.13}$$

where

$$E_{C3} = \frac{1}{E_1(k)} \times \left[\frac{1}{k} - k + \frac{(V_1 - V_2)^2 \left(\rho_1 \mu_2^2 M_0(k) (N_0(k) + N_2(k))^2 + \rho_2 \mu_1^2 N_0(k) (M_0(k) + M_2(k))^2 \right)}{(\mu_1 (M_0(k) + M_2(k)) + \mu_2 (N_0(k) + N_2(k)))^2} \right].$$

When $\mu_1 = \mu_2$, E_{C3} reduces to

$$\tilde{E}_{C3} = \frac{1}{E_1(k)}\left[\frac{1}{k} - k + \frac{(V_1 - V_2)^2(\rho_1 M_0(k)(N_0(k) + N_2(k))^2 + \rho_2 N_0(k)(M_0(k) + M_2(k))^2)}{(M_0(k) + M_2(k) + N_0(k) + N_2(k))^2}\right].$$

Once more, we return to the general case. This case is actually defined by equation (4.4), which describes the dispersion relation of the interface among two cylindrical Rivlin–Ericksen fluids. Using similar expression as given by (4.12), the system becomes linearly stable when

$$E_0^2 \geqslant E_{C4} \tag{4.14}$$

where

$$E_{C4} = \frac{1}{E_1(k)}\left[\frac{1}{k} - k + \frac{(V_1 - V_2)^2(C_{41} + C_{42})}{(\mu_1(M_0(k) + M_2(k)) + \mu_2(N_0(k) + N_2(k))^2}\right]$$

$$C_{41} = \mu_2^2(N_0(k) + N_2(k))^2(k^2\nu_1(M_0(k) + M_2(k)) + \rho_1 M_0(k))$$

and

$$C_{42} = \mu_1^2(M_0(k) + M_2(k))^2(k^2\nu_2(N_0(k) + N_2(k)) + \rho_2 N_0(k)).$$

It is worthwhile to note that the streaming has a destabilizing influence in all special cases as well as the general one. In the absence of streaming, in all special cases as well as the general one, the linear stability criterion is reduced to

$$E_0^2 \geqslant E_C \tag{4.15}$$

where

$$E_C = \frac{1}{E_1(k)}\left(\frac{1}{k} - k\right).$$

Therefore, we recover the well-known result which states that the jet is always stable when $kR > 1$ [27, 30].

In what follows, we shall make a numerical estimation for the stability picture for the surface waves propagating between two cylindrical Rivlin–Ericksen fluids. In order to screen this examination, numerical calculations for the transition curves (4.8), (4.10), (4.13) and (4.14) are made for the variation of the electric field intensity versus the wave number. The points of the marginal stability lie on these transition curves which separate the stable from unstable regions. In the following figures the stable region is referred to by *S*, while *U* stands for the unstable one.

The special cases stated above are shown through figures 2, 3 and 4. The general case is plotted in figure 5. All the cases are shown in figures 6 and 7. In figure 6, the electric field intensity is shown versus the velocity difference $V = |V_1 - V_2|$ at constant value of the wave number $k = 0.25$ while in figure 7, the electric field intensity is plotted versus the wave number at constant value of the velocity difference $V = 4$.

In the stability diagram given in figure 2, we considered the transition curve (4.8). The system is considered as a pure inviscid fluid. As shown in the figure, the tangential electric field has a stabilizing influence, which is an early phenomenon observed by several authors [28]. It is also observed that the velocity difference has a destabilizing influence. Figure 3 screens the transition curve (4.10). As can be seen in this figure, the transition curves change their behaviour, so that the instability is enhanced. Therefore, the presence of the viscoelastic coefficients has a destabilizing influence. It is also observed that the role of the streaming is unchanged. Similar curves as in figure 2 are observed in figure 4, where the transition curves (4.13) are plotted. One can say that the viscosity coefficients have an opposite influence than the viscoelastic coefficients. The general case is plotted in figure 5. Therefore, the transition

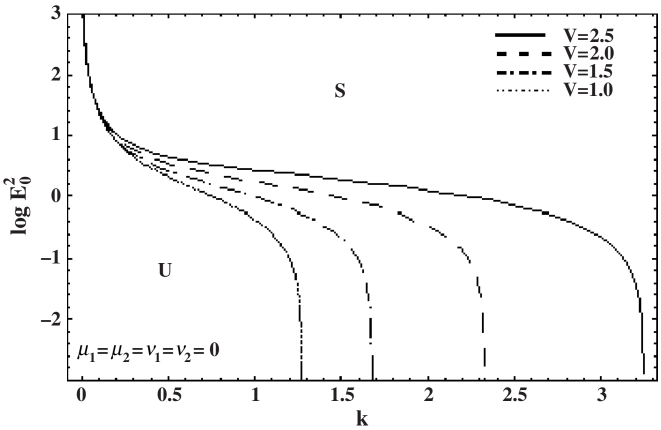

Figure 2. Stability diagram in view of the linear stability theory for a system having the particulars: $\rho_1 = 1.0$, $\rho_2 = 0.879$, $\varepsilon_1 = 2$, $\varepsilon_2 = 5$. The figure indicates the transition curve (4.8).

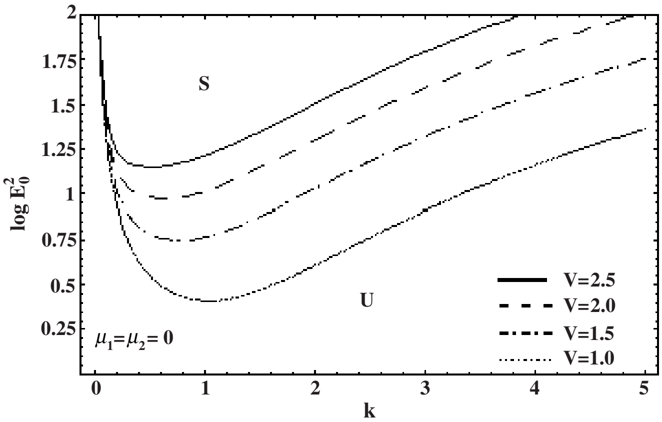

Figure 3. As in figure 2, but when $\nu_1 = 1$ and $\nu_2 = 2$. The figure indicates the transition curve (4.10).

curves (4.14) are plotted. It is found that the behaviour of these curves is similar to that in figure 3. This similarity is due to the presence of the viscoelastic coefficients. Figure 6 includes all cases. Therefore, all the transition curves (4.8), (4.10), (4.12) and (4.14) are shown in this figure. In this figure, all curves represent parabolas. The inspection of figure 7 shows that the stability is enhanced in the absence of the parameters μ_1, μ_2, ν_1 and ν_2. Also, ν_1 and ν_2 are more effective than μ_1 and μ_2, where the transition curves change their behaviour, so that the system becomes more destabilizing. At large values of k, the parameters μ_1 and μ_2 have no effect, where the transition curves (4.10) and (4.14) coincide. The influence of μ_1 and μ_2 appear at small values of k.

5. The derivation of the Ginzburg–Landau equation

To investigate the non-linear stability of the considered system, we may introduce a modulation to the problem so that the linear dispersion relation $S(w, k)$ represents a slowly modulated wave train. To do this, we may use an expansion procedure based on the method of multiple

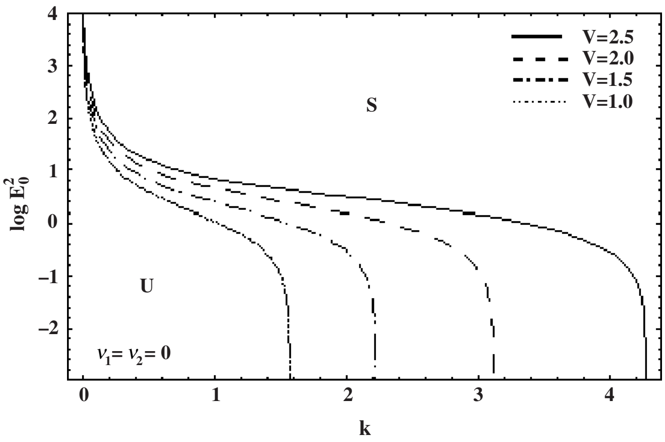

Figure 4. As in figure 2, but when $\mu_1 = 1$ and $\mu_2 = 2$. The figure indicates the transition curve (4.13).

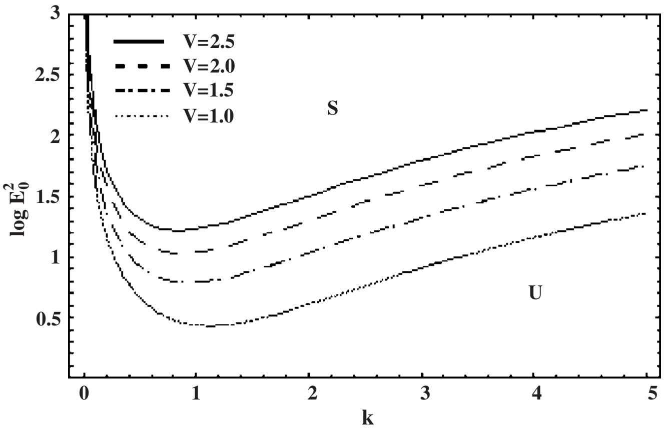

Figure 5. As in figure 2, but when $\mu_1 = 1$, $\mu_2 = 2$, $\nu_1 = 1$ and $\nu_2 = 2$. The figure indicates the transition curve (4.14).

scale [32]. The underlying idea of the method of multiple scales is to make an expansion representing the solution of a problem not only as a function of one independent variable, but also as a function of two or more independent variables which are referred to as scales. We shall assume a small parameter δ which measures the ratio of a typical wavelength or periodic time relative to a typical length or timescale of the modulation (measures the Steppes ratio as the perturbation parameter). The independent variables z and t, which are measured on scale of a typical wavelength and periodic time, may be extended to introduce alternative independent variables,

$$T_n = \delta^n t \qquad Z_n = \delta^n z \qquad n = 1, 2. \tag{5.1}$$

Thus defining T_0, Z_0 as variables appropriate to fast variations, T_1, T_2, Z_1 and Z_2 are slow variables. The differential operators can be expressed as derivative expansions

$$\frac{\partial}{\partial t} \equiv -\omega \frac{\partial}{\partial \theta_0} + \delta \frac{\partial}{\partial T_1} + \delta^2 \frac{\partial}{\partial T_2} \cdots \tag{5.2}$$

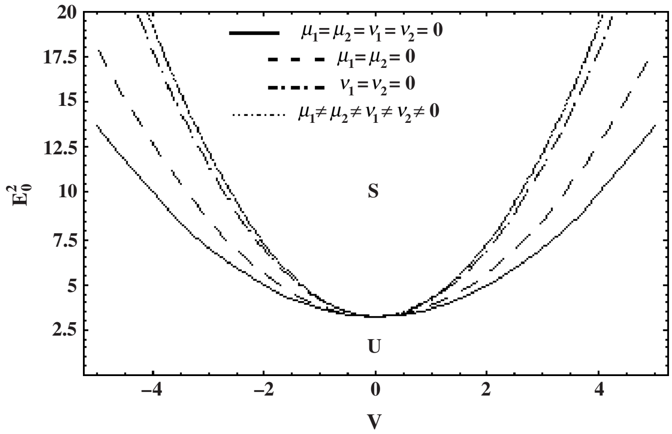

Figure 6. As in figure 5, but when $k = 0.25$, and for various values of V.

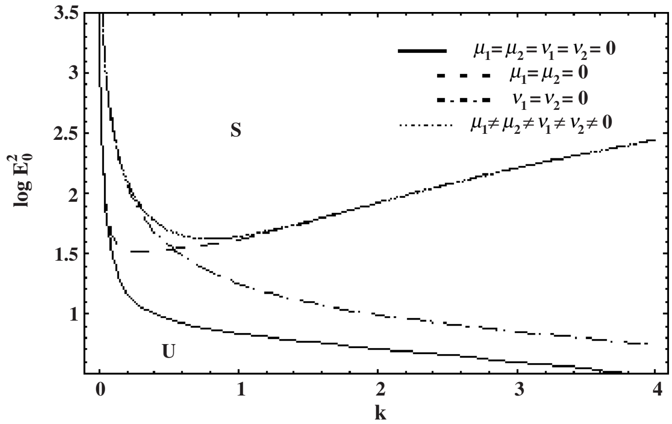

Figure 7. As in figure 6, but when $V = 4$. The figure indicates the transition curves (4.8), (4.10), (4.13) and (4.14).

$$\frac{\partial}{\partial z} \equiv -k\frac{\partial}{\partial \theta_0} + \delta\frac{\partial}{\partial Z_1} + \delta^2\frac{\partial}{\partial Z_2} \cdots \tag{5.3}$$

where $\theta_0 = kZ_0 - \omega T_0$, T_0 and Z_0 are the lowest orders of the time and the phase of oscillations of the wave train.

The analysis follows through a perturbation procedure and the suppression of the secular terms is now more convenient to write a uniformly valid solution. The procedure was introduced in details by Moatimid [13].

It is well known that the non-linear Schrödinger equation is a generic equation describing unidirectional wave modulation. It has been used to describe the spatial and temporal evolution of the envelope of a sinusoidal wave with phase $(kz - \omega t)$, drawing potential energy from some background field. Following similar arguments as given by Moatimid [13], one finds the Ginzburg–Landau equation

$$\mathrm{i}\frac{\partial \gamma}{\partial \tau} + (P_r + \mathrm{i}P_i)\frac{\partial^2 \gamma}{\partial \xi^2} = (Q_r + \mathrm{i}Q_\mathrm{i})\gamma^2\bar{\gamma} \tag{5.4}$$

where $\bar{\gamma}$ denotes the complex conjgate of γ,

$$Q_r + \mathrm{i}Q_i = \left(\frac{2\alpha^2}{\Omega} + \beta\right)\left(\frac{\partial S}{\partial \omega}\right)^{-1}$$

$$P_r + \mathrm{i}P_i = -\frac{1}{2}\left[V_g^2 \frac{\partial^2 S}{\partial \omega^2} + 2V_g \frac{\partial^2 S}{\partial \omega \partial k} + \frac{\partial^2 S}{\partial k^2}\right]\left(\frac{\partial S}{\partial \omega}\right)^{-1}$$

$$\xi = \delta(z - V_g t) \qquad \text{and} \qquad \tau = \delta^2 t.$$

in which the group velocity V_g is given by

$$V_g = -\left(\frac{\partial S}{\partial k}\right)\left(\frac{\partial S}{\partial \omega}\right)^{-1}$$

and the non-zero denominator Ω may be derived from the dispersion function $S(\omega, k)$ by replacing both ω and k with 2ω and $2k$, respectively. The vanishing of the denominator refers to the second harmonic resonance. In general, the harmonic resonance may exist if (ω, k) and $(n\omega, nk)$, where n is a positive integer, satisfy the same dispersion relation [32].

Equation (5.4) is derived from the non-linear system (3.7). The complex coefficients $P_r + \mathrm{i}P_i$ and $Q_r + \mathrm{i}Q_i$ are constructed in terms of the linear dispersion relation (4.4) which is of complex nature. This equation is a standard non-linear Ginzburg–Landau equation. It may be used to study the stability behaviour of the considered system. Lange and Newell [34] derived the stability criteria of this equation. If the solution of equation (5.4) is linearly perturbed, the perturbations are stable if both the following conditions

$$Q_i < 0 \tag{5.5}$$

$$P_r Q_r + P_i Q_i > 0 \tag{5.6}$$

are satisfied. Otherwise, the system is unstable (i.e. the system does not oscillate about its equilibrium state). The absence of the imaginary parts P_i and Q_i in the above criteria is reduced to those obtained by Nayfeh [12] and others. The transition curves separating the stable from the unstable region correspond to

$$Q_i = 0 \tag{5.7}$$

$$P_i Q_i + P_r Q_r = 0. \tag{5.8}$$

These marginal curves may be born out of numerical estimation. Before proceeding to the numerical calculations for the stability profile, it is convenient to write the transition curves (5.7) and (5.8) in appropriate dimensionless forms. Consider the same dimensionless form as presented in (4.8). At this end, the stability can, therefore, be discussed by dividing the $\left(E_0^2 - k\right)$ plane into stable and unstable regions. After lengthy but straightforward calculations, the transition curve $Q_i = 0$ may be arranged in a third-degree polynomial on E_0^2 as

$$A_0\left(E_0^2\right)^3 + A_1\left(E_0^2\right)^2 + A_2\left(E_0^2\right) + A_3 = 0 \tag{5.9}$$

while the transition curve $P_i Q_i + P_r Q_r = 0$ may be arranged in a fifth-degree polynomial on E_0^2 as

$$B_0\left(E_0^2\right)^5 + B_1\left(E_0^2\right)^4 + B_2\left(E_0^2\right)^3 + B_3\left(E_0^2\right)^2 + B_4\left(E_0^2\right) + B_5 = 0 \tag{5.10}$$

where A and B are functions on all the parameters defined in figure 1. To aid readers to have a better understanding of the theory and its derivation, these coefficients are given in appendix B.

The next step in the analysis of the jet instability is to determine the stable and unstable regions through the non-linear theory, for example, the behaviour of the electric field in the

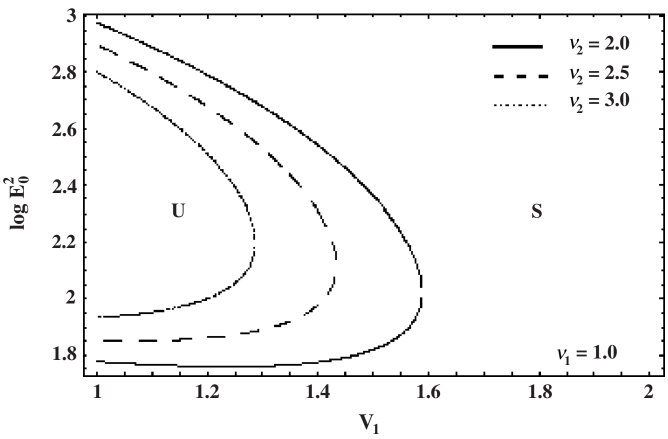

Figure 8. Stability diagram in view of the non-linear stability approach for a system having the particulars: $\rho_1 = 1.0$, $\rho_2 = 0.879$, $\varepsilon_1 = 2$, $\varepsilon_2 = 5$, $\mu_1 = 1$, $\mu_2 = 2$, $k = 0.4$, $V_2 = 1$, $\nu_1 = 1$ and for various values of ν_2.

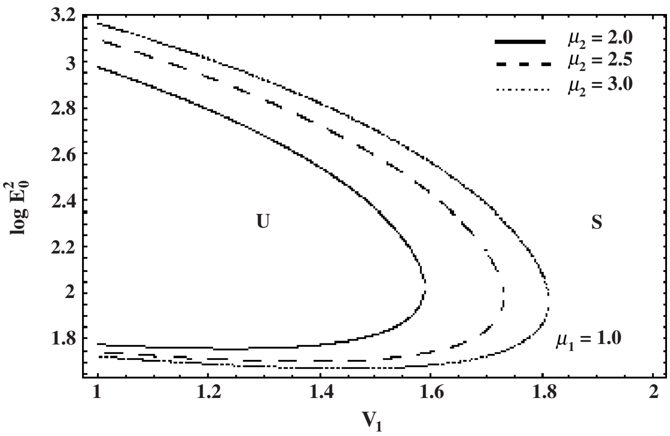

Figure 9. As in figure 8, but when $\nu_2 = 2$ and for various values of μ_2.

parameter space. In what follows, we shall consider the linear and the non-linear stability criteria through figures 8 and 9. In the following figures, we try to compute all the transition curves in the linear and non-linear approaches. Therefore, we compute the transition curves (4.14), (5.9) and (5.10) through these figures for some sample chosen system at a single value of the wave number ($k = 0.4$). In the light of the linear theory, the transition curve (4.14) disappeared in these figures. It follows that the system becomes stable in the light of the linear theory. Through the non-linear approach, we try to calculate all the roots of the transition curves (5.9) and (5.10). It is found that the stability is controlled by the transition curve $Q_i = 0$. Furthermore, two roots only from (5.9) govern the stability of the system. The inspection of these curves shows that the non-linear effects partition the stable region into stable and unstable parts. From figure 8, we observe that the parameter ν_2 has a stabilizing influence. This is in contrast to the linear theory. An opposite role of the parameter μ_2 is seen in figure 9, where μ_2 has a destabilizing influence.

Through the non-linear approach, the second harmonics of the fundamental disturbance (the phenomenon of this resonance arises because of the occurrence of the singularity of the non-linear term in the Ginzburg–Landau equation (5.4)) is mainly responsible for the formation of the satellite drops. It is, therefore, expected that the satellite drop formation can be controlled by using frequency modulated disturbances [35]. The newly generated disturbances or the higher harmonic may be stable if their wave number is larger than the cut-off wave number. Therefore, a better understanding of the behaviour of the electric jet subject to disturbances with wave numbers larger than the cut-off wave number (i.e. stable region) can help in explaining the influence of the higher harmonic on the jet instability and in designing disturbances to better control the jet break-up process.

6. Concluding remarks

In the present work, a weak non-linear scope is performed in order to investigate the surface wave instability between two cylindrical viscoelastic fluids in the presence of a tangential electric fluid. No surface charges at the cylindrical interface are assumed. Also, in the stationary state, the fluids uniformly stream parallel to each other. Because of the great importance of the practical applications of the viscoelastic cylindrical fluids, we consider a Rivlin–Ericksen model. The viscoelasticity is revealed through the parameters μ and ν.

The analysis for the linear theory as presented by Chandrasekhar [27] is based on neglecting the non-linear terms from the equations of motion as well as the boundary conditions, and then imposing a dispersion relation without non-linear terms. The idea for this weak non-linear description is a slight departure from the linear point of view. At this end, the non-linear problem will contain linear description with some additional terms representing a correction to the main solution. The weakly non-linear description given here is based on neglecting the non-linear terms from the equations of motion and applying the appropriate boundary conditions without dropping the non-linear terms. At this end, a dispersion relation arises with the non-linear terms to become the characteristic equation of the problem.

The present boundary-value problem leads to a non-linear characteristic equation. This equation has complex coefficients of the elevation function. The non-linearity is kept up to the third order. The method of multiple scales in spatial and temporal developments is used. By making use of the Taylor expansion to obtain uniformly valid solutions of the characteristic equation, we obtain the well-known Ginzburg–Landau equation. This equation describes the elevation of the wave train up to the third order. From the non-linear stability analysis, we have obtained the transition curves $Q_i = 0$ and $P_r Q_r + P_i Q_i = 0$. They are rearranged, to be plotted in the $\left(E_0^2 - V\right)$ plane, in third and fifth degrees in E_0^2, respectively. Based on the modelling results, several conclusions can be made as follows:

(1) In the linear stability analysis, the neutral stability curve that partitions the parameter space into two different regions states that:
   - (i) The relative streaming velocity V has a destabilizing influence in the general case as well as in all special cases.
   - (ii) The viscoelastic coefficient ν has a destabilizing influence. It has a stronger effect than the viscosity coefficient μ.
   - (iii) The viscosity coefficient μ has its dominant influence at small values of k.

(2) The non-linear numerical calculations considered some sample chosen system at a fixed value of the wave number $k = 0.4$ as a numerical example. It is observed that the stable region, in the light of the linear theory, is partitioned into stable and unstable parts. Also, in contrast to the linear theory, we found that ν_2 has a stabilizing influence. Therefore, the viscoelastic coefficient ν has a dual role in the stability criterion.

Appendix A

The coefficients of the non-linear terms appearing in the characteristic equation (3.7) are given by

$$\begin{aligned}
\alpha(\omega,k) = k\Bigg\{&\frac{1}{2}\big[k^2\nu_1\big(-11+4M_0^2(kR)+4M_0(kR)M_2(kR)-M_3(kR)\big)-2\rho_1M_0^2(kR)\\
&-k^2\nu_2\big(-11+4N_0^2(kR)+4N_0(kR)N_2(kR)-N_3(kR)\big)-2\rho_2N_0^2(kR)\big]\omega^2\\
&-k\big[V_1\big(k^2\nu_1\big(-11+4M_0^2(kR)+4M_0(kR)M_2(kR)-M_3(kR)\big)+2\rho_1M_0^2(kR)\big)\\
&-V_2\big(k^2\nu_2\big(-11+4N_0^2(kR)+4N_0(kR)N_2(kR)-N_3(kR)\big)+2\rho_2N_0^2(kR)\big)\\
&+\mathrm{i}k\big(\mu_1\big(4+M_0^2(kR)-M_0(kR)M_2(kR)\big)+\mu_2\big(-4+N_0^2(kR)\\
&-N_0(kR)N_2(kR)\big)\big)\big]\omega+\frac{T}{2R^3}(2+k^2R^2)+k^2E_2(kR)E_0^2+\frac{1}{2}k^2V_1^2\\
&\times\big[k^2\nu_1\big(-11+4M_0^2(kR)+4M_0(kR)M_2(kR)-M_3(kR)\big)+2\rho_1M_0^2(kR)\big]\\
&-\frac{1}{2}k^2V_2^2\big[k^2\nu_2\big(-11+4N_0^2(kR)+4N_0(kR)N_2(kR)-N_3(kR)\big)\\
&+2\rho_2N_0^2(kR)\big]-\mathrm{i}k^3\big[\mu_1V_1\big(-4+M_0^2(kR)+M_0(kR)M_2(kR)\big)\\
&-\mu_2V_2\big(-4+N_0^2(kR)+N_0(kR)N_2(kR)\big)\big]\Bigg\}
\end{aligned}$$

$$\begin{aligned}
\beta(\omega,k) = k^2\Bigg\{&\big[k^2\nu_1\big(3M_2(kR)\big(1+M_0^2(kR)\big)+M_0(kR)\big(-6+3M_0^2(kR)-M_3(kR)\big)\big)\\
&+\rho_1M_0^3(kR)+k^2\nu_2\big(3N_2(kR)\big(1+N_0^2(kR)\big)+N_0(kR)\big(-6+3N_0^2(kR)\\
&+N_2(kR)-N_3(kR)\big)\big)+\rho_2N_0^3(kR)\big]\omega^2+k\big[2V_1\big(k^2\nu_1\big(M_0(kR)\big(-6\\
&+3M_0^2(kR)-M_3(kR)\big)+3M_2(kR)\big(1+M_0^2(kR)\big)\big)+\rho_1M_0^3(kR)\big)\\
&+2V_2\big(k^2\nu_2\big(N_0(kR)\big(-6+3N_0^2(kR)-N_3(kR)\big)+3N_2(kR)\big(1+N_0^2(kR)\big)\big)\\
&+\rho_2N_0^3(kR)\big)-\mathrm{i}k\big(\mu_1\big(-M_0(kR)\big(1-M_0^2(kR)\big)+M_2(kR)\big(1+M_0^2(kR)\big)\big)\\
&+\big(\mu_2\big(-N_0(kR)\big(1-N_0^2(kR)\big)+N_2(kR)(1+N_0^2(kR))\big)\big)\big)\big]\omega\\
&-\frac{T}{2kR^4}(2+k^2R^2-3k^4R^4)-k^3E_3(kR)E_0^2\\
&-k^2\big[V_1^2\big(k^2\nu_1\big(M_0(kR)\big(-6+3M_0^2(kR)-M_3(kR)\big)\\
&+3M_2(kR)\big(1+M_0^2(kR)\big)\big)+\rho_1M_0^3(kR)\big)+V_2^2\big(k^2\nu_2\big(N_0(kR)\\
&\times\big(-6+3N_0^2(kR)-N_3(kR)\big)+3N_2(kR)\big(1+N_0^2(kR)\big)\big)+\rho_1N_0^3(kR)\big)\big]\\
&+\mathrm{i}k^3\big(\mu_1V_1\big(M_0(kR)\big(-1+M_0^2(kR)\big)+M_2(kR)\big(1+M_0^2(kR)\big)\big)\\
&+\mu_2V_2\big(N_0(kR)\big(-1+N_0^2(kR)\big)+N_2(kR)\big(1+N_0^2(kR)\big)\big)\big)\Bigg\}
\end{aligned}$$

$$E_1(kR) = \frac{(\varepsilon_1-\varepsilon_2)^2M_0(kR)N_0(kR)}{\varepsilon_1N_0(kR)+\varepsilon_2M_0(kR)}$$

$$\begin{aligned}
E_2(kR) = &\frac{(\varepsilon_1-\varepsilon_2)^2}{2(\varepsilon_1N_0(kR)+\varepsilon_2M_0(kR))^2}\\
&\times\big[\varepsilon_1N_0^2(kR)\big(3M_0^2(kR)-1\big)-\varepsilon_2M_0^2(kR)\big(3N_0^2(kR)-1\big)\big]
\end{aligned}$$

$$E_3(kR) = \frac{(\varepsilon_1-\varepsilon_2)^2M_0(kR)N_0(kR)}{(\varepsilon_1N_0(kR)+\varepsilon_2M_0(kR))^3}\big\{\varepsilon_1^2N_0^2(kR)\big(2M_0^2(kR)-1\big)$$

$$+\varepsilon_1\varepsilon_2\big[N_0^2(kR)\big(1-M_0^2(kR)\big)+M_0(kR)N_0(kR)+M_0^2(kR)\big(1-N_0^2(kR)\big)\big]$$
$$+\varepsilon_2^2M_0^2(kR)\big(2N_0^2(kR)-1\big)\big\}$$

with

$$M_j=\frac{I_j(kR)}{I_1(kR)}\qquad\text{and}\qquad N_j=\frac{K_j(kR)}{K_1(kR)}\qquad j=0,2,3,\ldots.$$

Appendix B

Consider the following parameters:

$$M=\frac{I_0(k)}{I_1(k)}\qquad\text{and}\qquad Mj=\frac{I_j(k)}{I_1(k)}\qquad j=2,3,4,$$
$$K=\frac{K_0(k)}{K_1(k)}\qquad\text{and}\qquad Kj=\frac{K_j(k)}{K_1(k)}\qquad j=2,3,4,$$
$$F=\frac{MK(\varepsilon_1-\varepsilon_2)^2}{K\varepsilon_1+M\varepsilon_2}$$
$$x_1=-2(k^2(M+M2)(-1+kV_1)\nu_1+k^2(K+K2)(-1+kV_2)\nu_2$$
$$+M(-1+kV_1)\rho_1+K(-1+kV_2)\rho_2)$$
$$y_1=k^2((M+M2)\mu_1+(K+K2)\mu_2)$$
$$x_{21}=\frac{F}{2(K\varepsilon_1+M\varepsilon_2)^2}(k(\varepsilon_1-\varepsilon_2)^2(K^2(-4M+k(-2+M(M+M2)))\varepsilon_1$$
$$-(4K+k(-2+K(K+K2)))M^2\varepsilon_2))$$
$$x_{22}=\tfrac{1}{2}(2-6k^2-k(-1+kV_1)(4(M+M2)-k(-3+(M+M2)^2-M3)$$
$$+k(-8(M+M2)+k(-3+(M+M2)^2-M3))V_1)\nu_1$$
$$+k(-1+kV_2)(-4(K+K2)-k(-3+(K+K2)^2-K3)$$
$$+k(8(K+K2)+k(-3+(K+K2)^2-K3)V_2)\nu_2$$
$$-(-1+kV_1)(2-M(M+M2)+(-4M+k(-2+M(M+M2)))V_1)\rho_1$$
$$+(-2+K(K+K2))\rho_2+V_2(-2(2K+k(-2+K(K+K2)))$$
$$+k(4K+k(-2+K(K+K2)))V_2)\rho_2)$$
$$y_2=\tfrac{1}{2}k((4(M+M2)-k(-3+(M+M2)^2-M3)+k(-6(M+M2)$$
$$+k(-3+(M+M2)^2-M3))V_1)\mu_1+(4(K+K2)$$
$$+k(-3+(K+K2)^2-K3)-k(6(K+K2)$$
$$+k(-3+(K+K2)^2-K3))V_2)\mu_2)$$
$$x_3=2(k^2(M+M2)\nu_1+M\rho_1+k^2(K+K2)\nu_2+K\rho_2)$$

$g_{11}=-x_1x_{21}$ $\quad g_{12}=-(x_1x_{22}+y_1y_2)$ $\quad g_{21}=x_{21}y_1$ $\quad g_{22}=x_{22}y_1-x_1y_2$

$g_{31}=g_{11}^2-g_{21}^2$ $\quad g_{32}=2(g_{11}g_{12}-g_{21}g_{22})$ $\quad g_{33}=g_{12}^2-g_{22}^2$

$g_{41}=2g_{11}g_{21}$ $\quad g_{42}=2(g_{12}g_{21}+g_{11}g_{22})$ $\quad g_{43}=2g_{12}g_{22}$

$x_{41}=g_{31}x_3$ $\quad x_{42}=g_{33}x_3$ $\quad x_{43}=g_{33}x_3$

$y_{41}=g_{41}x_3$ $\quad y_{42}=g_{42}x_3$ $\quad y_{43}=g_{43}x_3$

$$x_5=k(4(M+M2)-k(-3+(M+M2)^2-M3)+k(-6(M+M2)$$
$$+k(-3+(M+M2)^2-M3))V_1)\nu_1-k(-4(K+K2)$$
$$-k(-3+(K+K2)^2-K3)+k(6(K+K2)+k(-3+(K+K2)^2-K3))V_2)\nu_2$$

$$+(2-M(M+M2)+(-2M+k(-2+M(M+M2)))V_1)\rho_1$$
$$-(2-K(K+K2)+(2K+k(-2+K(K+K2)))V_2)\rho_2$$

$$y_5=\tfrac{1}{2}k((4(M+M2)-k(-3+(M+M2)^2-M3))\mu_1+(4(K+K2)$$
$$-k(-3+(K+K2)^2-K3))\mu_2)$$

$$x_{61}=2(g_{11}x_5-g_{21}y_5) \qquad x_{62}=2(g_{12}x_5-g_{22}y_5)$$
$$y_{61}=2(g_{21}x_5+g_{11}y_5) \qquad y_{62}=2(g_{22}x_5+g_{12}y_5)$$

$$x_{71}=-\frac{F}{4(K\varepsilon_1+M\varepsilon_2)^3}((\varepsilon_1-\varepsilon_2)^2(K^3(8M+k(16-8M(M+M2)$$
$$+k(-2M2+M(-5+2(M+M2)^2-M3))))\varepsilon_1^2$$
$$-(-16K^2M^2+8kKM(2M+K(-2+M(-K-K2+M+M2)))$$
$$+k^2(8M^2+4K^3M(-2+(M+M2))-2KM(3K2M$$
$$+4(-2+M(M+M2)))+K^2(8+M(-6M2+4K2(-2+M(M+M2))$$
$$+M(-6+K3+M3)))))\varepsilon_1\varepsilon_2+M^3(8K+k(-16+8K(K+K2)$$
$$+k(-2K2+K(-5+2(K+K2)^2-K3))))\varepsilon_2^2$$

$$x_{72}=\tfrac{1}{4}(-24k+(8(M+M2)+k(-8(M+M2)^2+8(3+M3)$$
$$+k(-5M2+2(M^3+3M^2M2+M2^3+3M(-1+M2^2))$$
$$-3(M+M2)M3+M4))+kV_1(-2(24(M+M2)+k(-12(M+M2)^2$$
$$+12(3+M3)+k(-5M2+2(M^3+3M^2M2+M2^3+3M(-1+M2^2))$$
$$-3(M+M2)M3+M4)))+k(48(M+M2)+k(-16(M+M2)^2$$
$$+16(3+M3)+k(-5M2+2(M^3+3M^2M2+M2^3+3M(-1+M2^2))$$
$$-3(M+M2)M3+M4)))V_1))\nu_1+(8(K+K2)+k(8(-3+(K+K2)^2-K3)$$
$$+k^2(-5K2+2(K^3+3K^2K2+K2^3+3K(-1+K2^2))-3(K+K2)K3+K4))$$
$$+kV_2(-2(24(K+K2)+12k(-3+(K+K2)^2-K3)$$
$$+k^2(-5K2+2(K^3+3K^2K2+K2^3+3K(-1+K2^2))$$
$$-3(K+K2)K3+K4))+k(48(K+K2)+16k(-3+(K+K2)^2-K3)$$
$$+k^2(-5K2+2(K^3+3K^2K2+K2^3+3K(-1+K2^2))$$
$$-3(K+K2)K3+K4))V_2))\nu_2+(-2M2+M(-5+2(M+M2)^2-M3)$$
$$+V_1(2(-8+4M(M+M2)+k(2M2+M(5-2(M+M2)^2+M3)))$$
$$+(8M+k(16-8M(M+M2)+k(-2M2+M(-5+2(M+M2)^2$$
$$-M3))))V_1))\rho_1+(-2K2+K(-5+2(K+K2)^2-K3)$$
$$-2(-8+4K(K+K2)+k(-2K2+K(-5+2(K+K2)^2-K3)))V_2$$
$$+\big(8K+k\big(-16+8K(K+K2)+k(-2K2$$
$$+K(-5+2(K+K2)^2-K3))))V_2^2\big)\rho_2\big)$$

$$y_7=\tfrac{1}{4}((8(M+M2)+k(-8(M+M2)^2+8(3+M3)+k(-5M2+2(M^3+3M^2M2+M2^3$$
$$+3M(-1+M2^2))-3(M+M2)M3+M4))-k(24(M+M2)$$
$$+k(-12(M+M2)^2+12(3+M3)+k(-5M2+2(M^3+3M^2M2$$
$$+M2^3+3M(-1+M2^2))-3(M+M2)M3+M4)))V_1)\mu_1+(8(K+K2)$$
$$+k(8(-3+(K+K2)^2-K3)+k(-5K2+2(K^3+3K^2K2+K2^3$$
$$+3K(-1+K2^2))-3(K+K2)K3+K4))-k(24(K+K2)$$

$$+k(12(-3+(K+K2)^2-K3)+k(-5K2+2(K^3+3K^2K2+K2^3 +3K(-1+K2^2))-3(K+K2)K3+K4)))V_2)\mu_2)$$

$x_{81}=x_{41}$ $\quad x_{82}=x_{42}+\left(x_1^2+y_1^2\right)\left(x_{61}+x_{71}\left(x_1^2+y_1^2\right)\right)$

$x_{83}=x_{43}+\left(x_1^2+y_1^2\right)\left(x_{62}+x_{72}\left(x_1^2+y_1^2\right)\right)$ $\quad y_{81}=y_{41}$ $\quad y_{82}=y_{42}+\left(x_1^2+y_1^2\right)y_{61}$

$y_{83}=y_{43}+\left(x_1^2+y_1^2\right)\left(y_7\left(x_1^2+y_1^2\right)+y_{62}\right)$

$P_{R1}=-(x_1x_{81}+y_1y_{81})$ $\quad P_{R2}=-(x_1x_{82}+y_1y_{82})$ $\quad P_{R3}=-(x_1x_{83}+y_1y_{83})$

$P_{I1}=-x_1y_{81}+y_1x_{81})$ $\quad P_{I2}=y_1x_{82}-x_1y_{82}$ $\quad P_{I3}=-x_1y_{83}+y_1x_{83}$

$$a=\frac{I_0(2k)}{I_1(2k)}\quad b=\frac{I_2(2k)}{I_1(2k)}\quad c=\frac{K_0(2k)}{K_1(2k)}\quad d=\frac{K_2(2k)}{K_1(2k)}$$

$$G_1=\frac{ac(\varepsilon_1-\varepsilon_2)^2}{c\varepsilon_1+a\varepsilon_2}\quad G_2=\frac{(\varepsilon_1-\varepsilon_2)^2((3M^2-1)K^2\varepsilon_1+(-3K^2+1)M^2\varepsilon_2)}{2(K\varepsilon_1+M\varepsilon_2)^2}$$

$$G_3=\left\{MK(\varepsilon_1-\varepsilon_2)^2\left((2M^2-1)K^2\varepsilon_1^2+(K^2(1-M^2)+MK+M^2(1-K^2))\varepsilon_1\varepsilon_2 +(2K^2-1)M^2\varepsilon_2^2\right)\right\}\big/(K\varepsilon_1+M\varepsilon_2)^3$$

$\Omega_{11}=-4k^2G_1$ $\quad \Omega_{31}=2\Omega_{11}^2$ $\quad \Omega_{32}=4\Omega_{11}\Omega_{12}$ $\quad \Omega_{33}=2\Omega_{12}^2$ $\quad \alpha_{11}=k^3G_2$

$$\Omega_{12}=2(k-4k^3+2(4(a+b)k^2(-1+kV_1)^2\nu_1+4(c+d)k^2(-1+kV_2)^2\nu_2 +a(-1+kV_1)^2\rho_1+c(-1+kV_2)^2\rho_2))$$

$$\Omega_2=-8k^2((a+b)(-1+kV_1)\mu_1+(c+d)(-1+kV_2)\mu_2)$$

$$\alpha_{12}=\tfrac{1}{2}k(2+k^2+k^2(-11+4M(M+M2)-M3)(-1+kV_1)^2\nu_1 -k^2(-11+4K(K+K2)-K3)(-1+kV_2)^2\nu_2 +2M^2(-1+kV_1)^2\rho_1-2K^2(-1+kV_2)^2\rho_2)$$

$$\alpha_2=k^3(-(-4+M(M+M2))(-1+kV_1)\mu_1+(-4+K(K+k2))(-1+kV_2)\mu_2)$$

$\alpha_{31}=\alpha_{11}^2$ $\quad \alpha_{32}=2\alpha_{11}\alpha_{12}$ $\quad \alpha_{33}=-\alpha_2^2+\alpha_{12}^2$

$\alpha_{41}=2\alpha_2\alpha_{11}$ $\quad \alpha_{42}=2\alpha_2\alpha_{12}$ $\quad \beta_{11}=-k^4G_3$

$$\beta_{12}=-k^4(3M2+M(-6+3M(M+M2)-M3))(-1+kV_1)^2\nu_1-\tfrac{1}{2}k(2+k^2-3k^4 +2k(k^2(3K2+K(-6+3K(K+K2)-K3))(-1+kV_2)^2\nu_2 +M^3(-1+kV_1)^2\rho_1+K^3(-1+kV_2)^2\rho_2))$$

$$\beta_2=k^4((M2+M(-1+M(M+M2)))(-1+kV_1)\mu_1 +(K2+K(-1+K(K+K2)))(-1+kV_2)\mu_2)$$

$\alpha_{51}=\alpha_{11}\alpha_{31}$ $\quad \alpha_{52}=\alpha_{11}\alpha_{32}+\alpha_{31}\Omega_{12}$ $\quad \alpha_{53}=\alpha_{11}\alpha_{33}+\alpha_{41}\Omega_2+\alpha_{32}\Omega_{12}$

$\alpha_{54}=\alpha_{42}\Omega_2+\alpha_{33}\Omega_{12}$ $\quad \alpha_{61}=\alpha_{11}\alpha_{41}-\alpha_{31}\Omega_2$ $\quad \alpha_{62}=\alpha_{11}\alpha_{42}-\alpha_{32}\Omega_2+\alpha_{41}\Omega_{12}$

$\alpha_{63}=-\alpha_{33}\Omega_2+\alpha_{42}\Omega_{12}$ $\quad \beta_{31}=2\alpha_{51}+\beta_{11}\Omega_{31}$ $\quad \beta_{32}=2\alpha_{52}+\beta_{12}\Omega_{31}+\beta_{11}\Omega_{32}$

$\beta_{33}=2\alpha_{53}+\beta_{12}\Omega_{32}+\beta_{11}\Omega_{33}$ $\quad \beta_{34}=2\alpha_{54}+\beta_{12}\Omega_{33}$ $\quad \beta_{41}=2\alpha_{61}+\beta_2\Omega_{31}$

$\beta_{42}=2\alpha_{62}+\beta_2\Omega_{32}$ and $\beta_{43}=2\alpha_{63}+\beta_2\Omega_{33}$.

Therefore, the coefficients of the transition curves appearing in equation (5.9) are given by

$A_0=-y_1\beta_{31}$ $\quad A_1=-y_1\beta_{32}+x_1\beta_{41}$ $\quad A_2=-y_1\beta_{33}+x_1\beta_{42}$

and $A_3=-y_1\beta_{34}+x_1\beta_{43}$.

Now, consider the following additional parameters:

$Q_{R1}=x_1\beta_{31}$ $\quad Q_{R2}=x_1\beta_{32}+y_1\beta_{41}$ $\quad Q_{R3}=x_1\beta_{33}+y_1\beta_{42}$ $\quad Q_{R4}=x_1\beta_{34}+y_1\beta_{43}$.

Therefore, the coefficients of the transition curves appearing in equation (5.10) are given by

$$B_0 = P_{I1}A_0 + P_{R1}Q_{R1} \qquad B_1 = P_{I2}A_0 + P_{I1}A_1 + P_{R1}Q_{R1} + P_{R1}Q_{R2}$$
$$B_2 = P_{I3}A_0 + P_{I2}A_1 + P_{I1}A_2 + P_{R3}Q_{R1} + P_{R2}Q_{R2} + P_{R1}Q_{R3}$$
$$B_3 = P_{I3}A_1 + P_{I2}A_2 + P_{I1}A_3 + P_{R3}Q_{R2} + P_{R2}Q_{R3} + P_{R1}Q_{R4}$$
$$B_4 = P_{I3}A_2 + P_{I2}A_3 + P_{R3}Q_{R3} + P_{R2}Q_{R4}$$

and

$$B_5 = P_{I3}A_3 + P_{R3}Q_{R4}.$$

References

[1] Winslow W M 1949 *J. Appl. Phys.* **20** 1137
[2] Perez A T, Vazques P A and Castellanos A 1995 *IEEE. Trans. Ind. Appl.* **31** 761
[3] Gonzalez A and Castellanos A 1997 *J. Electrost.* **40** 55
[4] Koulova-Nebova D and Atten P 1997 *J. Electrost.* **40** 185
[5] Feng J Q and Beard K V 1991 *J. Fluid Mech.* **222** 417
[6] Moatimid G M 2001 *Chaos, Solitons Fractals* **12** 1239
[7] Moatimid G M 2002 *J. Colloid. Interface Sci.* **250** 108
[8] El-Dib Y O and Moatimid G M 2002 *Z. Naturforsch.* **57a** 159
[9] Moatimid G M 2003 *J. Colloid. Interface Sci.* **259** 186
[10] El-Sayed M F 2002 *Chaos, Solitons Fractals* **14** 1137
[11] El-Dabe N T, Moatimid G M and Ali H S M 2002 *Z. Naturforsch.* **57a** 863
[12] Nayfeh A H 1976 *J. Appl. Mech. (Trans. ASME)* **98** 584
[13] Moatimid G M 2003 *Z. Angew. Math. Phys.* at press
[14] Othman M I A 1998 *Z. Angew. Math. Phys.* **49** 759
[15] Lee D-S 2002 *Eur. Phys. J.* B **28** 495
[16] Lee D-S 2002 *Z. Angew. Math. Mech.* **82** 567
[17] Lee D-S 2002 *Z. Naturforsch.* **57a** 682
[18] Elhefnawy A R F, Moatimid G M and Elcoot A K 2003 *Phys. Scripta* **67** 513
[19] Elhefnawy A R F, Moatimid G M and Elcoot A K 2003 *Can. J. Phys.* **81** 805
[20] Elhefnawy A R F, Moatimid G M and Elcoot A K 2003 *Z. Angew. Math. Phys.* at press
[21] Rosenau P and Oron A 1989 *Phys. Fluids* A **1** 1753
[22] Davalos-Orozco L A and Ruiz-Chavarria G 1993 *Phys. Fluids* A **5** 2390
[23] Hung C I, Chen C K and Tasi J S 1996 *Int. J. Heat Mass Transfer* **39** 2821
[24] Cheng P J, Chen C K and Lai H Y 2001 *J. Fluid Eng.* **123** 411
[25] Melcher J R 1963 *Field Coupled Surface Waves* (Cambridge, MA: MIT)
[26] Batchelor G K 1997 *An Introduction to Fluid Dynamics* (Cambridge: Cambridge University Press)
[27] Chandrasekhar S 1961 *Hydrodynamic and Hydromagnetic Stability* (Oxford: Oxford University Press)
[28] Moatimid G M 1995 *Int. J. Eng. Sci.* **33** 119
[29] Grimshaw R H J 1981 *Wave Motion* **3** 81
[30] Rayleigh L 1945 *The Theory of Sound* vol II (New York: Dover)
[31] Zahreddine Z and El-Shehawey E F 1988 *Indian J. Pure Appl. Math.* **19** 963
[32] Nayfeh A H and Mook D T 1979 *Nonlinear Oscillation* (Virginia: Wiley)
[33] Elhefnawy A R F 1992 *Physica* A **182** 419
[34] Lange C G and Newell A C 1974 *SIAM J. Appl. Math.* **27** 441
[35] Ashgrize A and Mashayek F 1995 *J. Fluid Mech.* **291** 163